



Trichomes affect grapevine leaf optical properties and thermoregulation

Corrado Domanda · Vitale Nuzzo ·
Giuseppe Montanaro · Osvaldo Failla ·
Laura Rustioni

Received: 6 March 2023 / Accepted: 15 August 2023
© The Author(s) 2023

Abstract In the context of climate change, the optical properties of grapevine leaves have been used in imaging technologies to screen grapevine phenotypes tolerant to water deficit and heat waves in field conditions. Image-based plant phenotyping is challenging because the adaxial and the abaxial sides of the leaf present different morphology. This study investigated the effect of trichomes of the abaxial epidermis on the spectral responses in the two grapevine leaf sides. It was also examined the effect of pubescence on leaf

thermoregulation, either during water deficiency or not. For this study, 99 *Vitis spp.* genotypes were categorised for their prostrate trichome density between main veins on the abaxial side of the leaves (using the descriptor OIV 084). In the first week of 2022, August, reflectance spectra from 400 to 700 nm and color indexes CIELAB and RGB were recorded in five leaves (both abaxial and adaxial sides) per genotype. During three days in midsummer, crop water stress index (CWSI) was also determined in each genotype. The abaxial leaf side was more reflective than the adaxial one in all visible color bands. Values of CIELAB (except for component a*) and RGB were higher for the abaxial leaf side than the adaxial one. The different spectral and color responses between leaf sides positively correlated with the descriptor OIV 084. Trichomes, which mainly occur on the abaxial side in grapevine, significantly contribute to the different optical properties between the two leaf sides. Correlation between OIV 084 and CWSI values was significantly positive ($p < 0.05$) only when vines were under drought, indicating that trichomes rise leaf temperature by probably reducing evaporative cooling under dry conditions. Therefore, pubescence could be a promising trait to consider when selecting varieties for drought tolerance.

Supplementary Information The online version contains supplementary material available at <https://doi.org/10.1007/s40626-023-00287-z>.

C. Domanda (✉) · L. Rustioni
Department of Biological and Environmental Sciences and Technologies, University of Salento, 73100 Lecce, Italy
e-mail: corrado.domanda@unisalento.it

L. Rustioni
e-mail: laura.rustioni@unisalento.it

V. Nuzzo · G. Montanaro
Università degli Studi della Basilicata, 85100 Potenza, Italy
e-mail: vitale.nuzzo@unibas.it

G. Montanaro
e-mail: giuseppe.montanaro@unibas.it

O. Failla
Department of Agricultural and Environmental Science, University of Milan, 20133 Milan, Italy
e-mail: osvaldo.failla@unimi.it

Keywords Abiotic stress · Ampelography · Boundary layer · Canopy temperature · Prostrate trichomes · Viticulture

1 Introduction

The optical properties of leaves are widely used in smart and precision viticulture. There is an increasing availability of proximal and remote sensing technologies based on imaging methods: RGB, infrared thermography, chlorophyll fluorescence, multispectral and hyperspectral, light detection and ranging (LiDAR). RGB imaging has been used to estimate the whole plant leaf area in grapevines (Coupel-Ledru et al. 2014). RGB-based imaging might be a promising tool to monitor water deficiency in grapevines, through vine water consumption and leaf angle estimations (Briglia et al. 2019, 2020). Grapevine water status can also be estimated by infrared thermography using thermal indexes, such as the crop water stress index (CWSI) (Jones 1992). Thermography is not strictly linked to the optical properties of a surface. Nevertheless, it is included in the imaging methodologies because, as Möller et al. (2007) reported, thermal images, in conjunction with visible and near-infrared (NIR) images, enable the exclusion of non-leaf material in the estimate of canopy temperature and the possibility of selecting specific parts of the canopy for water stress estimation. Plant susceptibility to generic abiotic stress can be evaluated by measuring chlorophyll fluorescence (Su et al. 2015). This method can be performed directly via chlorophyll fluorescence induction (CFIN) (Kautsky and Hirsh 1931), or chlorophyll fluorescence imaging (CFI) (Omasa et al. 1987; Daley et al. 1989). Briefly, CFIN is a point measurement, where the signal is collected by an optical fiber in close proximity to the leaf (Carvalho et al. 2021); CFI, instead, can collect whole-plant images and, thus, provides a huge amount of data which can be thoroughly analysed and used for early detection of plant stress (Humplík et al. 2015; Carvalho et al. 2021). Chlorophyll fluorescence can be also indirectly measured by multispectral and hyperspectral imaging applying two indices based on reflectance measurements, R690/R600 and R740/R800, that have been used to track changes in chlorophyll fluorescence (Dobrowski et al. 2005). Another application of multispectral and hyperspectral imaging are the vegetation indices such as the normalised difference vegetation index (NDVI), which is highly correlated with vine vigour (Costa Ferreira et al. 2007). Lastly, LiDAR technology was proven to successfully estimate the leaf area index by emitting

short-wavelength lasers in near-infrared light (Arnó et al. 2013). LiDAR sensors, however, can also emit in the visible or ultraviolet division of the electromagnetic spectrum (Lin 2015).

All these imaging methodologies can be relevant to characterize grapevine germplasm in field conditions for yield/quality or tolerance to abiotic stress and to support decisions in vineyard management (Carvalho et al. 2021). However, these authors consider that deepening and clarifying the link between the indirect digital measurements obtained by sensors and the morphological, eco-physiological, and metabolic parameters under examination would be necessary.

The optical properties vary depending on the different structures and chemical composition of the analysed surface. In grapevine, the two sides of the leaf are different. The mesophyll is asymmetric between the two sides, being the palisade parenchyma close to the adaxial leaf side and the spongy parenchyma near the abaxial one (Keller 2020). The palisade parenchyma consists of one or two layers of column-shaped cells with small intercellular spaces (MacMillan et al. 2021). The spongy parenchyma consists of four to six layers of irregularly shaped and loosely packed cells, with larger intercellular spaces (Keller 2020). The palisade tissue tends to occupy around 40% of the total mesophyll and the spongy tissue around 60%, but this proportion varies among genotypes (MacMillan et al. 2021). Both cell types contain large numbers of chloroplasts. In the palisade parenchyma, calcium oxalate crystals (Keller 2020) are aggregated to form octahedral crystals called druses. He et al. (2014) suggested that druses can distribute the incoming sunlight to the near chloroplasts, thus optimising photosynthesis. So, the presence of druses in the palisade parenchyma could contribute to the optical properties of the leaf adaxial side. The epidermis and the cuticle were found to be different between sides as well. Boso et al. (2010), by comparing seven genotypes of *Vitis spp.* (six being *Vitis vinifera* and the other *Vitis riparia*) demonstrated that all adaxial epidermis cells were convex and polygonal. Abaxial epidermis cells just in *V. vinifera* genotype ‘Syrah’ displayed instead greater variability within the three types observed: rounded polygonal cells, elongated polygonal cells, and sinuous cells (MacMillan et al. 2021). Boso

et al. (2010) reported that the cuticle of the abaxial side was thinner than in the adaxial side with stomata located almost exclusively in the abaxial epidermis. Finally, characteristic hairs called trichomes are found mainly in the abaxial epidermis of *V. vinifera* leaves (Monteiro et al. 2013).

The number and the length of trichomes are characteristic of each genotype and can be used in ampelography to discriminate among species and genotypes. Two types of grapevine non-glandular leaf trichomes, 'erect' and 'prostrate', are found (Gago et al. 2016), and the relative abundance and spatial density of each trichome type vary among grapevine genotypes. The main functions ascribed to trichomes in grapevine are the defence against downy mildew (Kortekamp and Zyprian 1999), the shelter for phytoseiid mites (Karban et al. 1995), and the tolerance to abiotic stresses (Keller 2020). Concerning the last point, trichomes affect water balance of plants by modulating boundary layer thickness (Bickford 2016), acting like an extra-cuticular membrane that opposes resistance to water vapour diffusion and other gases through the leaf. Ripley et al. (1999) indicated that trichomes increase the boundary layer thickness and, consequently, the resistance to the water flow outside the leaf. Trichomes can thus reduce leaf transpiration rate, saving water for the plant (Ripley et al. 1999; Kenzo et al. 2008), however, the discussion is still ongoing (Bickford 2016). In addition, the effect of trichomes on leaf temperature is not always univocal. According to Peng et al. (2015), dense trichomes in *Eriophyton wallichii* can turn the leaves warmer up to 3 °C; on the other hand, in *Encelia farinosa*, trichomes lower the epidermal temperature by reflecting the amount of solar radiation absorbed by the leaves (Ehleringer 1988). Reflective trichomes may finally contribute to the different optical properties of the two sides of the grapevine leaf, giving the underside of some pubescent leaves a whitish appearance.

Based on such circumstances, the aim of this paper is to: (1) prove the difference of color between the two leaf sides of *Vitis spp.*; (2) investigate if pubescence in the abaxial leaf side is involved in the color difference between sides; (3) explore if any correlation exists between trichome density and grapevine thermoregulation, particularly during drought periods.

2 Material and methods

2.1 Experimental design

The experiment was carried out in August 2022 in a private collection of *Vitis spp.* germplasm. The collection was located in the Salento viticultural area (Apulia Region, Southern Italy). The vineyard was planted in a plain area (Latitude 40.35, Longitude 17.40, Elevation 25 m a.s.l.). Plants were spaced 2.2 m (inter-row) and 0.9 m (in-row), with a plant density of about 5,000 plants ha⁻¹. Vines were trained at classic spur cordon; soil was managed by tillage, and the vineyard was equipped with an irrigation system. No additional water was supplied during the experimental period.

Ninety-nine *Vitis spp.* genotypes of different geographical origins were considered casually in the collection. All the selected genotypes consisted of six vines planted each. For each genotype, in the first week of August, five mature leaves were collected from the six vines and the density of prostrate trichomes on the abaxial side of the leaf determined according to the recommendations of OIV (OIV 2009). Briefly, the visual observation of the density of prostrate trichomes was made in the region between main veins of the entire abaxial leaf side (OIV 084 descriptor), applying a categorical value from 1 (lowest density) to 9 (highest density). Concerning the leaf position on the shoot, only the sixth or seventh node was considered, depending on the leaf integrity. Immediately after pubescence description, on the same five leaves/genotype, reflectance spectra (R) from 400 to 700 nm (± 10 nm accuracy) and the value of the RGB and CIELAB coordinates were recorded for both the abaxial and adaxial sides. The RGB (Red, Green, Blue) color model describes components of a color in relation to the standardized reference wavelengths of monochromatic red, green, and blue lights (Ly et al. 2020). Instead, the CIELAB (or CIEL*a*b*) color space, which was standardized in 1976 by the Commission Internationale de l'Eclairage (CIE), is a three-dimensional color space consisting of three axes. L* expresses the human perceptual lightness of a surface and it is represented on a vertical axis with values from 0 (black) to 100 (white). The a* coordinate indicates red-green component of a color, where positive a* and negative a* indicate red and green values, respectively. The yellow and blue

components are represented on the b^* axis as positive b^* and negative b^* values, respectively (Ly et al. 2020). In this work, a total of 990 reflectance spectra and color measurements were obtained. The R, RGB and CIELAB values were measured avoiding the main leaf veins using a portable colorimeter ‘Spectro 1’ (Variable Inc., Chattanooga, US) operating with a D65 10° light source. Each record was then directly saved in the related smartphone iOS app ‘Spectro by Variable’ (Variable Inc., Chattanooga, US). The reciprocal of the reflectance spectra ($1/R$) was used to approximate the (quasi)linear relationship between pigment content and optical reflectance-based indices, which is directly related to the absorbance properties of the surfaces. A similar elaboration approach was used by the authors considering different plant tissues (Rustioni et al. 2014, 2018; Rustioni and Bianchi 2021). Delta L^* index was calculated as the average difference for each genotype in L^* between abaxial and adaxial leaf sides.

On the same genotypes used for colorimetric and spectra measurements, the surface temperature of five mature shaded leaves/genotype was estimated with an infrared thermometer (Shenzhen Everbest Machinery Industry Co., Shenzhen, CN) between 11:00 and 14:00 h on 5th August, 17th August, and 30th August 2022. Overall, 1485 leaf temperature data were obtained. The order of temperature readings was randomly changed across genotypes each day. The temperatures of two artificial references (green rectangular 15×23.5 cm cards, with the following RGB values: R 47.6, G 65, B 56.4) placed together in the shade inside the canopy were also measured. One card was soaked with tap water every 10 min, being the wet reference (T_{wet}); the other card was left as dry as it was, being the dry reference (T_{dry}). Every 10 min, the surface temperature of both wet and dry references was recorded. CWSI was then calculated after Jones (1992) as follows:

$$CWSI = \frac{T_{\text{canopy}} - T_{\text{wet}}}{T_{\text{dry}} - T_{\text{wet}}}$$

where T_{canopy} was the actual leaf temperature, and T_{wet} and T_{dry} were the reference temperatures to mimic a fully transpiring leaf with open stomata and a non-transpiring leaf with closed stomata, respectively. Evidence of drought stress on 5th August, 17th August, and 30th August 2022 occurred if CWSI

daily average was higher than 0.7 (Bellvert et al. 2014).

2.2 Data analyses

A principal component analysis (PCA) was performed on all absorbance and colorimetric values in SPSS (IBM Corporation, Armond, US). A one-way analysis of variance (ANOVA) for the RGB and CIELAB values using the leaf side as factor was made in RStudio (Posit PBC, Boston, UK). Delta PC1 index was calculated as the average difference for each variety in component 1 PCA between the abaxial and adaxial leaf sides. Variables delta L^* , delta PC1 and CWSI were checked for normality of distribution using the Shapiro–Wilk test and the Kolmogorov–Smirnov test. As long as delta PC1, delta L^* , and CWSI were not normally distributed, correlations between OIV 084 and delta L^* , delta PC1 or CWSI were performed using the Spearman’s rank test. The relative contribution of the pubescence on leaf thermoregulation was estimated as percentage of variability of the CWSI explained by the OIV 084 records, calculated based on the ANOVA sum of the squares of the deviations from the mean.

3 Results

The $1/R$ reflectance average spectra of adaxial and abaxial leaf sides for all the genotypes are exhibited in Fig. 1 (first week of August, 2022). The yellow line in the figure indicates the difference between the two sides. For each wavelength recorded in the visible range, the abaxial leaf side reflects more radiation than the adaxial one. The net spectral difference between the two sides is always more than zero, both in the main maxima peaks (≈ 490 nm and ≈ 640 nm) and in the minimum peak at ≈ 570 nm. Standard error among all 99 genotypes is much lower than the difference between the two sides. The components of CIELAB color space and RGB color model were found to be higher for the abaxial leaf side than the adaxial one (Table 1), with the exception of the component a^* .

$1/R$ reflectance spectra of each leaf side were summarised by PCA (Fig. 2), with two principal components, explaining 95.3% of the total variability: 79.2% and 16.1% for PC1 (regression factor score 1) and

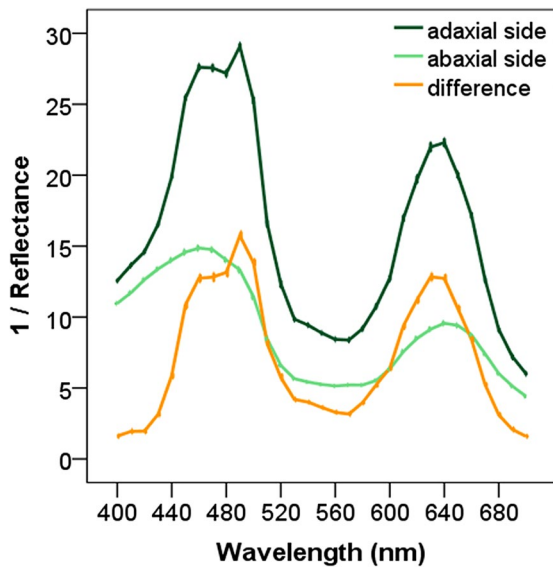


Fig. 1 Adaxial and abaxial leaf side average spectra and the net difference between them. Bars indicate the standard error, and their small size is due to the high number of measurements: the average values were calculated considering the 5 leaves of the ninety-nine *Vitis spp.* genotypes assessed in this work

Table 1 Components of the CIELAB color space and RGB color model in abaxial and adaxial leaf sides of ninety-nine genotypes of *Vitis spp*

Color space components	Abaxial side	Adaxial side
L*	47 ± 4.2 ^a	36.1 ± 4.6 ^b
a*	- 6.21 ± 1.5 ^a	- 6.04 ± 1.8 ^a
b*	24.1 ± 5 ^a	17.5 ± 8.4 ^b
R	115.2 ± 12.1 ^a	85.3 ± 13 ^b
G	113.5 ± 10.4 ^a	87.2 ± 11.2 ^b
B	69.7 ± 7.7 ^a	55.7 ± 6.5 ^b

L*, lightness; +a* (positive) or -a* (negative), red or green values, respectively; +b* (positive) or -b* (negative), yellow or blue values, respectively; R, red component; G, green component; B, blue component. Average values and standard deviations are reported. Different letters in the same row represent significantly different means by one-way ANOVA with post-hoc test Bonferroni ($p < 0.05$)

PC2 (regression factor score 2), respectively. In Supplementary materials, it is possible to find a plot of the correlation values between each variable and PC1 and PC2 (Fig. s.1). PC1 highly correlates with almost the entire visible range (from 440 to 700 nm) (Fig.

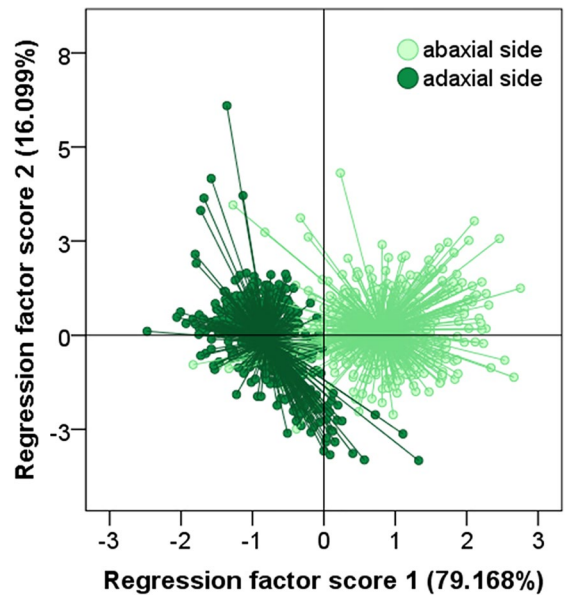


Fig. 2 Distribution of leaf side spectra based on the two principal components obtained by the PCA analysis of ninety-nine genotypes of *Vitis spp*

s.1A). Spectra variability distributed by PC1 on the X-axis can discriminate between the leaf sides: the adaxial side is located quite extensively to the left of the graph while the abaxial one to the right part of the graph (Fig. 2). PC2 highly correlates only with wavelengths from 400 to 430 nm (Fig. s.1B) and it does not discriminate properly with the leaf side (Fig. 2).

Table s.1 in Supplementary materials reports the categorical values of OIV 084 for each genotype selected for this work, as well as the VIVC code of the genotypes registered in the VIVC database. Fig. 3 shows the correlation between OIV 084 with delta L* and delta PC1 indexes (first week of August). Both correlations OIV 084 with delta L* and OIV 084 with delta PC1 are significant. Neither delta L* nor delta PC1 can discriminate significantly among the first three classes of OIV 084 but only for the top two classes. Correlation between OIV 084 and delta PC1 shows less standard deviation than the OIV 084 and delta L* one.

Considering the CWSI data, the daily average values recorded during the experiment were 0.72, 0.63, and 0.55, respectively, for 5th August, 17th August, and 30th August 2022, indicating the occurrence of drought only during the first

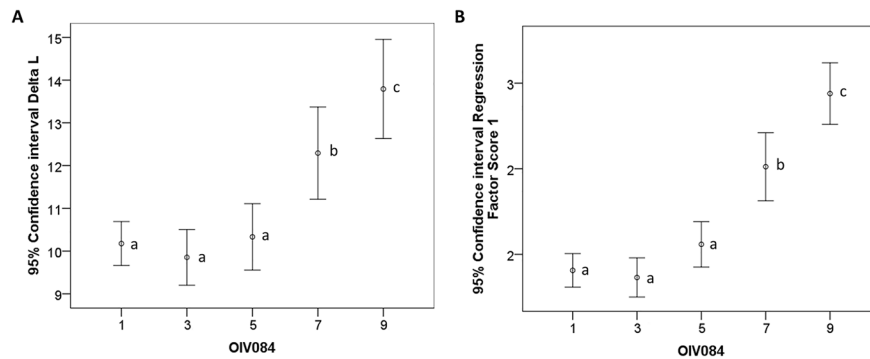


Fig. 3 **A** Correlation between ampelographic descriptor OIV 084 with delta L* index (Spearman's R 0.598, $p < 0.001$); **B** Correlation between OIV 084 and delta PC1 index (Spearman's R 0.417, $p < 0.001$). Ninety-nine genotypes of *Vitis spp.*

were considered for correlations **A** and **B**. Different letters represent significantly different means by one-way ANOVA with post-hoc test Duncan ($p < 0.05$). Bars indicate the standard deviation

experimental day. It is worth noting that, during 2022, many rainy events occurred in the second half of August in the experimental vineyard (data not shown).

The correlation between OIV 084 and CWSI was found to be significant, as well (Table 2). August 5th is the only day with a significant correlation between OIV 084 and CWSI. The relative contribution to the pubescence on the leaf thermoregulation is also reported in Table 2. Only a small part of the variability is explained by pubescence. Nevertheless, it should be noted that the contribution of trichomes to leaf thermoregulation is greater on the most stressful day (August 5th).

4 Discussion

Imaging methodologies have been used in recent years to screen grapevine germplasm and to support decisions in the vineyard management. However, until now, they cannot overcome the anatomical and physiological differences between the two leaf sides, at least in field conditions. For instance, we found that the leaf abaxial side is more reflective than the adaxial side all along the visible light division of the electromagnetic spectrum. This evidence cannot be ascribed to the high intraspecific variability used in this work because the standard error is negligible compared to the net difference due to the sides. Furthermore, the same result was obtained by performing a PCA on the 1/R of each leaf side (Fig. 2). The first component (PC1), which is highly correlated with almost the entire visible range (from

Table 2 Correlations between OIV 084 and CWSI (Significance code: *, $p < 0.05$; **, $p < 0.001$) considering ninety-nine genotypes of *Vitis spp*

CWSI—OIV 084	Total	Drought August, 5th	No drought	
			August, 17th	August, 30th
Spearman correlation coefficient	.058*	.179**	– .008	.034
Significance of the analysis (2-code)	.026	.000	.854	.452
Number of data considered for the analysis	1484	495	495	494
Percentage of variability of the CWSI explained by the OIV 084 records	1.62	7.77	2.21	2.73

Drought occurred only on August, 5th (CWSI daily average > 0.7), while no drought was observed on August, 17th and August, 30th (CWSI daily average < 0.7)

440 to 700 nm, see Fig. s.1A in Supplementary materials), does discriminate the leaf sides.

The highest discrepancy between sides is located at ≈ 490 nm and 640 nm, which are approximately the absorption regions of most photosynthetic pigments, mainly chlorophyll *b* and beta-carotene (Boyer 1990). The reflectance difference between leaf sides recorded in our study can be partially explained by the anatomy of the mesophyll tissues, palisade on the adaxial side, and spongy on the abaxial one. The interfaces between air and water at the intercellular spaces in the spongy mesophyll reflect and refract the incoming light, thus randomising its direction of progress. This phenomenon is known as interface light scattering, and it was theorised for the first time by Willstätter and Stoll (1918). Because of the interface light scattering, the abaxial side mesophyll cells are conducive to light reflection. Palisade cells on the adaxial side are instead much more packed, allowing the transmission of light into the leaf interior in a sort of light channelling mechanism. From an ecophysiological perspective, in this way plants absorb light more uniformly throughout the leaf. Interface light scattering and light channelling concur to explain why the components of CIELAB and RGB, except for a^* , were different between the two sides. The color component a^* was similar between sides because leaves were collected green as much as possible, trying to avoid any disease symptoms and far away from the leaf fall.

Nevertheless, the net I/R difference is not zero even in the 520–580 nm region, where chlorophyll does not absorb. Other biodiversity factors between sides, such as in the epidermal morphology, could also be implicated. Hu et al. (2021) investigated, for different grapevine genotypes, the spectral response of the adaxial and the abaxial leaf sides both in the visible band and in the near-infrared band. In the visible band, the reflectance of the leaf abaxial side was higher than the reflectance of the adaxial side, as in our case. On the contrary, in the near-infrared band, they found that the reflectance of the leaf adaxial side was higher than the reflectance of the abaxial side. The authors stated that the observed reflectance differences between leaf sides were due to not only the different structures of the mesophyll tissues but also the presence of stomata just in the leaf abaxial epidermis.

In *V. Vinifera*, pubescence is another morphological difference between leaf sides because trichomes are mainly on the abaxial side (Monteiro et al. 2013; Ma et al. 2016). Leaf trichomes are known to reflect broad-spectrum over the 400–700 nm visible range (Mershon et al. 2015). Thus, pubescence could most likely play a significant role in the observed variability between sides in reflectance and lightness. Indeed, significant linear correlations were found between trichome density (OIV 084) and delta PC1 and delta L* (Fig. 3). The correlations were positive, meaning that, as pubescence becomes greater, reflectance and lightness increase. This trend is in accordance with Bickford (2016), who calculated (not for the genus *Vitis*) a 7% to 10% decrease in leaf reflectance of visible wavelengths after leaf depilation. Despite these correlations being significant, no significant difference was found among the first three OIV 084 classes (Fig. 3). Leaves with low or very low trichome density may exhibit spectral properties indistinguishable from glabrous leaves in the photosynthetically active wavelengths. Gausman and Cardenas (1973) concluded the same by comparing differences in spectrophotometrically measured reflectance, transmittance, and absorbance over the 500–2500 nm wavelength interval among terminal leaflets of densely pubescent, normal and glabrous soybean [*Glycine max* (L.) Merr.] lines.

Despite this, the ecophysiology of trichomes is not confined to the optical properties of leaves. Pubescence in plants affects leaf thermoregulation by increasing boundary layer resistance and reflecting light. These two mechanisms seem to be antagonistic: while the first one makes the leaf warmer by reducing the evaporative cooling, the latter lowers the leaf temperature by decreasing the amount of solar radiation absorbed. The overall effect of pubescence on grapevine leaf thermoregulation has not been investigated so far. In this work, we decided to investigate the trait (density of prostrate trichomes between main veins on the abaxial side of the leaf) that would be the most impacting on thermoregulation. We considered the prostrate trichomes because they belong to both the mesophyll area (which is more relevant for transpiration), and the vein tissue (Gago et al. 2016). Nevertheless, a contribution of erect trichomes could not be excluded. The CWSI has often been used as a remotely sensed indicator of plant water status because it is conceived as a normalised index able to

estimate the midday stem water potential (Poblete-Echeverría et al. 2017). Bellvert et al. (2014) reported 0.7 as the water stress threshold for CWSI in vines. The CWSI also provides a diagnosis of leaf thermoregulation, being highly correlated also with the leaf transpiration rate (Ru et al. 2020).

Independently of the three CWSI days, the correlation between pubescence and thermoregulation was significant, although only slightly positive (Table 2). The low value of the total R coefficient might be due to the inconsistent and not significant correlations between OIV 084 and CWSI on the days 17th August and 30th August 2022, in which no drought was observed in the experimental vineyard (CWSI daily average less than 0.7). Thus, if vines are not water stressed, the trichome-induced enhancement of the boundary layer thickness, although calculable, does not contribute significantly to the total leaf resistance in the water flow from mesophyll to the atmosphere. Similar results were also reported by Benz and Martin (2006) for some *Tillandsia* species. A significant correlation and a much higher R coefficient were found for the day 5th August 2022, the only one reported as a drought day (CWSI daily average \approx 0.72). The highly significant correlation suggests that when grapevines experience water deficiency periods, the trichome-induced increase of the boundary layer resistance is not negligible.

The positive value of the correlation indicates that pubescence might allow the plant to save water in the soil by reducing transpiration, but in this way it raises up leaf temperature. The trichome light reflectance effect on leaf temperature (Ehleringer 1988) was not pointed out, at least in our experimental conditions. The thickening of the boundary layer could possibly overcome it. Alternatively, the reflectance effect might not be so relevant in grapevine as much as in herbaceous plants such as *Encelia farinosa* does, because the solar radiation is less scattered by the adaxial leaf surface (which is mainly glabrous in *V. vinifera*) than the abaxial one.

Generally, plants face the rising vapour pressure deficit and drought through a number of different and complementary mechanisms (Grossiord et al. 2020). Within a safe range of water potentials ($\psi_{\text{stem}} > -1.5$ MPa), grapevines main drought responses are the reduction of transpiration (E), stomatal conductance (g_s), hydraulic conductance (K), photosynthesis, and fruit yield (Gambetta et al.

2020). Transpiration is controlled by g_s , which is in turn down regulated under drought by abscisic acid (ABA) signals coming from the roots, the stem and/or the leaves (Shatil-Cohen et al. 2011; Lovisolo et al. 2016). As water deficit increases, vines can also accumulate osmotically active solutes in leaf cells (*i.e.* osmotic adjustment) so that they are able to maintain turgor pressure and stomatal conductance (Bartlett et al. 2014). Probably, in this context, the presence and the abundance of trichomes are not the main factors responsible for the leaf thermoregulation, explaining a relatively low percentage of variability of the CWSI. Nevertheless, playing a small but significant role, pubescence could contribute, along with the other mechanisms, to the plant performances and leaf spectral response during stressful conditions, especially in high temperature and high light summertime. For example, the putative osmotic adjustment induced by drought was likely influenced by the genetic diversity of the examined OIV 084 groups (During 1984), and thus differentially contributed to changing leaf optical properties (Cotrozzi et al. 2020). However, this co-occurring factor in combination with trichome density remains to be specifically tested.

5 Conclusion

This study highlights that the optical differences between the grapevine leaf sides are also due to the presence of trichomes mainly located on the abaxial side. When grapevines are under drought, trichomes rise leaf temperature by probably reducing evaporative cooling. In this way, trichomes would prevent water loss from the plant under dry conditions. Future studies need to investigate the role of different types of trichomes (*e.g.* erect vs prostrate) in grapevine thermoregulation. The abundance of trichomes may be a trait to seek when selecting varieties for drought tolerance.

Acknowledgements The authors are grateful to Azienda Vitivinicola Claudio Quarta Vignaiolo (Lizzano, TA, Italy) for the access to the vineyard. Financial support: RIPARTI project—Regione Puglia.

Funding Open access funding provided by Università del Salento within the CRUI-CARE Agreement.

Declarations

Conflict of interest The authors declare no conflict of interest.

Open Access This article is licensed under a Creative Commons Attribution 4.0 International License, which permits use, sharing, adaptation, distribution and reproduction in any medium or format, as long as you give appropriate credit to the original author(s) and the source, provide a link to the Creative Commons licence, and indicate if changes were made. The images or other third party material in this article are included in the article's Creative Commons licence, unless indicated otherwise in a credit line to the material. If material is not included in the article's Creative Commons licence and your intended use is not permitted by statutory regulation or exceeds the permitted use, you will need to obtain permission directly from the copyright holder. To view a copy of this licence, visit <http://creativecommons.org/licenses/by/4.0/>.

References

- Arnó J, Escolà A, Vallès JM et al (2013) Leaf area index estimation in vineyards using a ground-based LiDAR scanner. *Precis Agric* 14:290–306. <https://doi.org/10.1007/s11119-012-9295-0>
- Bartlett MK, Zhang Y, Kreidler N, Sun S, Ardy R, Cao K, Sack L (2014) Global analysis of plasticity in turgor loss point, a key drought tolerance trait. *Ecol Lett* 17:1580–1590. <https://doi.org/10.1111/ele.12374>
- Bellvert J, Zarco-Tejada PJ, Girona J, Fereres E (2014) Mapping crop water stress index in a ‘Pinot-noir’ vineyard: comparing ground measurements with thermal remote sensing imagery from an unmanned aerial vehicle. *Precis Agric* 15:361–376. <https://doi.org/10.1007/s11119-013-9334-5>
- Benz BW, Martin CE (2006) Foliar trichomes, boundary layers, and gas exchange in 12 species of epiphytic Tillandsia (Bromeliaceae). *J Plant Physiol* 163:648–656. <https://doi.org/10.1016/j.jplph.2005.05.008>
- Bickford CP (2016) Ecophysiology of leaf trichomes. *Funct Plant Biol* 43:807–814. <https://doi.org/10.1071/FP16095>
- Boso S, Alonso-Villaverde V, Santiago JL et al (2010) Macro- and microscopic leaf characteristics of six grapevine genotypes (*Vitis spp.*) with different susceptibilities to grapevine downy mildew. *Vitis* 49:43–50. <https://doi.org/10.5073/vitis.2010.49.43-50>
- Boyer RF (1990) Isolation and spectrophotometric characterization of photosynthetic pigments. *Biochem Educ* 18:203–206. [https://doi.org/10.1016/0307-4412\(90\)90137-D](https://doi.org/10.1016/0307-4412(90)90137-D)
- Briglia N, Montanaro G, Petrozza A, Summerer S, Cellini F, Nuzzo V (2019) Drought phenotyping in *Vitis vinifera* using RGB and NIR imaging. *Sci Hortic*. <https://doi.org/10.1016/j.scienta.2019.108555>
- Briglia N, Williams K, Wu D et al (2020) Image-based assessment of drought response in grapevines. *Front Plant Sci*. <https://doi.org/10.3389/fpls.2020.00595>
- Carvalho LC, Gonçalves EF, Marques da Silva J, Costa JM (2021) Potential phenotyping methodologies to assess inter- and intravarietal variability and to select grapevine genotypes tolerant to abiotic stress. *Front Plant Sci*. <https://doi.org/10.3389/fpls.2021.718202>
- Costa Ferreira AM, Germain C, Homayouni S et al (2007) Transformation of aerial high resolution images in vine vigour maps at intrablock scale by semi automatic image processing. XVth International GESCO meeting, Porec
- Cotrozzi L, Peron R, Tuinstra MR, Mickelbart MV, Couture JJ (2020) Spectral phenotyping of physiological and anatomical leaf traits related with maize water status. *Plant Physiol* 184:1363–1377. <https://doi.org/10.1104/pp.20.00577>
- Coupeledru A, Lebon E, Christophe A et al (2014) Genetic variation in a grapevine progeny (*Vitis vinifera* L. cvs Grenache x Syrah) reveals inconsistencies between maintenance of daytime leaf water potential and response of transpiration rate under drought. *J Exp Bot* 65:6205–6218. <https://doi.org/10.1093/jxb/eru228>
- Daley PF, Raschke K, Ball JT, Berry JA (1989) Topography of photosynthetic activity of leaves obtained from video images of chlorophyll fluorescence. *Plant Physiol* 90:1233–1238. <https://doi.org/10.1104/pp.90.4.1233>
- Dobrowski SZ, Pushnik JC, Zarco-Tejada PJ, Ustin SL (2005) Simple reflectance indices track heat and water stress-induced changes in steady-state chlorophyll fluorescence at the canopy scale. *Remote Sens Environ* 97:403–414. <https://doi.org/10.1016/j.rse.2005.05.006>
- Düring H (1984) Evidence for osmotic adjustment to drought in grapevines (*Vitis vinifera* L.). *Vitis* 23:1–10. <https://doi.org/10.5073/vitis.1984.23.1-10>
- Ehleringer JR (1988) Comparative ecophysiology of *Encelia farinosa* and *Encelia frutescens* - I. energy balance considerations. *Oecologia* 76:553–561. <https://doi.org/10.1007/BF00397869>
- Gago P, Conéjero G, Martínez MC, Boso S, This P, Verdeil JL (2016) Microanatomy of leaf trichomes: opportunities for improved ampelographic discrimination of grapevine (*Vitis vinifera* L.) cultivars. *Aust J Grape Wine Res* 22:494–503. <https://doi.org/10.1111/ajgw.12226>
- Gambetta GA, Herrera JC, Dayer S, Feng Q, Hochberg U, Castellarin SD (2020) The physiology of drought stress in grapevine: towards an integrative definition of drought tolerance. *J Exp Bot* 71:4658–4676. <https://doi.org/10.1093/jxb/eraa245>
- Gausman HW, Cardenas R (1973) Light reflectance by leaflets of pubescent, normal, and glabrous soybean lines. *Agron J* 65:837–838
- Grossiord C, Buckley TN, Cernusak LA et al (2020) Plant responses to rising vapor pressure deficit. *New Phytol* 226:1550–1566. <https://doi.org/10.1111/nph.16485>
- He H, Veneklaas EJ, Kuo J, Lambers H (2014) Physiological and ecological significance of biomineralization in plants. *Trends Plant Sci* 19:166–174. <https://doi.org/10.1016/j.tplants.2013.11.002>
- Hu YW, Lu YL, Yang LP, Yang GS, Liu KY, Wang L (2021) Hyperspectral response characteristics and correlation analysis of grape leaf tissue structure. *J Plant Nutr Fertil* 27:1213–1221. <https://doi.org/10.11674/zwf.20571>

- Humplík JF, Lazár D, Husičková A, Spíchal L (2015) Automated phenotyping of plant shoots using imaging methods for analysis of plant stress responses - a review. *Plant Methods*. <https://doi.org/10.1186/s13007-015-0072-8>
- Jones HG (1992) *Plants and microclimate*. Cambridge University Press, Cambridge
- Karban R, English-Loeb G, Walker MA, Thaler J (1995) Abundance of phytoseiid mites on *Vitis* species: effects of leaf hairs, domatia, prey abundance and plant phylogeny. *Exp Appl Acarol* 19:189–197. <https://doi.org/10.1007/BF00130822>
- Kautsky H, Hirsh A (1931) Neue versuche zur kohleneureasimilation. *Naturwissenschaften* 19:964
- Keller M (2020) *The science of grapevines*. Academic Press, Cambridge
- Kenzo T, Yoneda R, Azani MA, Majid NM (2008) Changes in leaf water use after removal of leaf lower surface hairs on *Mallotus macrostachyus* (Euphorbiaceae) in a tropical secondary forest in Malaysia. *J for Res* 13:137–142. <https://doi.org/10.1007/s10310-008-0062-z>
- Kortekamp A, Zyprian E (1999) Leaf hairs as a basic protective barrier against downy mildew of grape. *J Phytopathol* 147:453–459. <https://doi.org/10.1046/j.1439-0434.1999.00409.x>
- Lin Y (2015) LiDAR: an important tool for next-generation phenotyping technology of high potential for plant phenomics? *Comput Electron Agric* 119:61–73. <https://doi.org/10.1016/j.compag.2015.10.011>
- Lovisollo C, Lavoie-Lamoureux A, Tramontini S, Ferrandino A (2016) Grapevine adaptations to water stress: new perspectives about soil/plant interactions. *Theor Exp Plant Physiol* 28:53–66. <https://doi.org/10.1007/s40626-016-0057-7>
- Ly BCK, Dyer EB, Feig JL, Chien AL, Del Bino S (2020) Research techniques made simple: cutaneous colorimetry: a reliable technique for objective skin color measurement. *J Invest Dermatol* 140:3–12. <https://doi.org/10.1016/j.jid.2019.11.003>
- Ma ZY, Wen J, Ickert-Bond SM, Chen LQ, Liu XQ (2016) Morphology, structure, and ontogeny of trichomes of the grape genus (*Vitis*, Vitaceae). *Front Plant Sci*. <https://doi.org/10.3389/fpls.2016.00704>
- MacMillan P, Teixeira G, Lopes CM, Monteiro A (2021) The role of grapevine leaf morphoanatomical traits in determining capacity for coping with abiotic stresses: a review. *Cienc Tec Vitivinic* 36:75–88. <https://doi.org/10.1051/ctv/ctv2021360175>
- Mershon JP, Becker M, Bickford CP (2015) Linkage between trichome morphology and leaf optical properties in New Zealand alpine *Pachycladon* (Brassicaceae). *N Z J Bot* 53:175–182. <https://doi.org/10.1080/0028825X.2015.1042486>
- Möller M, Alchanatis V, Cohen Y et al (2007) Use of thermal and visible imagery for estimating crop water status of irrigated grapevine. *J Exp Bot* 58:827–838. <https://doi.org/10.1093/jxb/erl115>
- Monteiro A, Teixeira G, Lopes CM (2013) Comparative leaf micromorphoanatomy of *Vitis vinifera* SSP. *Vinifera* (Vitaceae) red cultivars. *Cienc Tec Vitivinic* 28:19–28
- OIV (2009) Second edition of the OIV descriptor list for grape varieties and *Vitis* species. <https://www.oiv.int/public/medias/2274/code-2e-edition-finale.pdf>. Accessed 27 Feb 2023
- Omasa K, Shimazaki KI, Aiga I, Larcher W, Onoe M (1987) Image analysis of chlorophyll fluorescence transients for diagnosing the photosynthetic system of attached leaves. *Plant Physiol* 84:748–752. <https://doi.org/10.1104/pp.84.3.748>
- Peng DL, Niu Y, Song B, Chen JG, Li ZM, Yang Y, Sun H (2015) Woolly and overlapping leaves dampen temperature fluctuations in reproductive organ of an alpine Himalayan forb. *J Plant Ecol* 8:159–165. <https://doi.org/10.1093/jpe/rtv014>
- Poblete-Echeverría C, Espinace D, Sepúlveda-Reyes D, Zúñiga M, Sanchez M (2017) Analysis of crop water stress index (CWSI) for estimating stem water potential in grapevines: comparison between natural reference and baseline approaches. *Acta Hort* 1150:189–194. <https://doi.org/10.17660/ActaHortic.2017.1150.27>
- Ripley BS, Pammenter NW, Smith VR (1999) Function of leaf hairs revisited: the hair layer on leaves *Arctotheca populifolia* reduces photoinhibition, but leads to higher leaf temperatures caused by lower transpiration rates. *J Plant Physiol* 155:78–85. [https://doi.org/10.1016/S0176-1617\(99\)80143-6](https://doi.org/10.1016/S0176-1617(99)80143-6)
- Ru C, Hu X, Wang W, Ran H, Song T, Guo Y (2020) Evaluation of the crop water stress index as an indicator for the diagnosis of grapevine water deficiency in greenhouses. *Horticulturae* 6:1–19. <https://doi.org/10.3390/horticulturae6040086>
- Rustioni L, Bianchi D (2021) Drought increases chlorophyll content in stems of *Vitis* interspecific hybrids. *Theor Exp Plant Physiol* 33:69–78. <https://doi.org/10.1007/s40626-021-00195-0>
- Rustioni L, Rocchi L, Guffanti E, Cola G, Failla O (2014) Characterization of grape (*Vitis vinifera* L.) berry sunburn symptoms by reflectance. *J Agric Food Chem* 62:3043–3046. <https://doi.org/10.1021/jf405772f>
- Rustioni L, Grossi D, Brancadoro L, Failla O (2018) Iron, magnesium, nitrogen and potassium deficiency symptom discrimination by reflectance spectroscopy in grapevine leaves. *Sci Hortic* 241:152–159. <https://doi.org/10.1016/j.scienta.2018.06.097>
- Shatil-Cohen A, Attia Z, Moshelion M (2011) Bundle-sheath cell regulation of xylem-mesophyll water transport via aquaporins under drought stress: a target of xylem-borne ABA? *Plant J* 67:72–80. <https://doi.org/10.1111/j.1365-3113X.2011.04576.x>
- Su L, Dai Z, Li S, Xin H (2015) A novel system for evaluating drought-cold tolerance of grapevines using chlorophyll fluorescence. *BMC Plant Biol*. <https://doi.org/10.1186/s12870-015-0459-8>
- Willstätter R, Stoll A (1918) *Untersuchungen über die assimilation der Kohlensäure*. Springer, Berlin

Publisher's Note Springer Nature remains neutral with regard to jurisdictional claims in published maps and institutional affiliations.